



City Research Online

City, University of London Institutional Repository

Citation: Bilotta, E. and Stallebrass, S. E. (2009). Prediction of stresses and strains around model tunnels with adjacent embedded walls in overconsolidated clay. *Computers and Geotechnics*, 36(6), pp. 1049-1057. doi: 10.1016/j.compgeo.2009.03.015

This is the accepted version of the paper.

This version of the publication may differ from the final published version.

Permanent repository link: <https://openaccess.city.ac.uk/id/eprint/4294/>

Link to published version: <http://dx.doi.org/10.1016/j.compgeo.2009.03.015>

Copyright: City Research Online aims to make research outputs of City, University of London available to a wider audience. Copyright and Moral Rights remain with the author(s) and/or copyright holders. URLs from City Research Online may be freely distributed and linked to.

Reuse: Copies of full items can be used for personal research or study, educational, or not-for-profit purposes without prior permission or charge. Provided that the authors, title and full bibliographic details are credited, a hyperlink and/or URL is given for the original metadata page and the content is not changed in any way.

Prediction of stresses and strains around model tunnels with adjacent embedded walls in overconsolidated clay

Emilio Bilotta ^{a,*}, Sarah E Stallebrass ^b

^a *Dipartimento di Ingegneria Idraulica, Geotecnica e Ambientale. Università di Napoli Federico II. Via Claudio, 21. 80125 Naples, Italy. Phone: +39 081 7683617. Fax: +39 081 7683481. E-mail: bilotta@unina.it (* corresponding author)*

^b *School of Engineering and Mathematical Sciences. City University London, Northampton Square, EC1V 0HB, London, UK.*

Abstract: This paper presents the results of finite element analyses carried out using different constitutive models for overconsolidated clay: the Modified Cam clay model and the Three-surface kinematic hardening (3-SKH) model. These analyses are evaluated against data from an extensive series of physical model tests examining the influence of an embedded wall placed near a tunnel on ground movements and tunnel stability. It is shown that for heavily overconsolidated soils reasonable predictions of both deformations and failure can be obtained from kinematic hardening models such as the 3-SKH model, which allow plastic deformation inside a Modified Cam clay state boundary surface.

Keywords: *Tunnelling, numerical analysis, constitutive models, overconsolidated soil*

1. Introduction

The prediction of realistic patterns of ground movement is a challenging issue in the finite element analysis of tunnel excavation. In particular, the accurate simulation of tunnelling in high- K_0 overconsolidated clays is still a problem, which has not yet been resolved¹. The ability of constitutive models based in the framework of Critical State

Soil Mechanics to predict the behaviour of these soils has been improved by the introduction of a kinematic yield surface inside the Modified Cam clay yield surface^{2, 3}. Indeed, kinematic hardening has become increasingly popular in the last decade as it has allowed small-strain non-linearity and the effects of stress path direction and recent stress history to be dealt with in a sound constitutive framework. Nevertheless, many issues need still to be addressed in this field: among others the evidence that the large strain response predicted for overconsolidated clay can be significantly influenced by the small strain formulation of the constitutive model.

This paper discusses the results of selected analyses in order to compare the performance of two different constitutive models for soil: the Modified Cam clay model⁴ and the Three-Surface Kinematic Hardening (3-SKH) model^{5, 6} in the solution of a relatively complex boundary value problem.

A series of finite element analyses were performed to study the behaviour of a diaphragm wall embedded in the ground close to where a tunnel is subsequently excavated. Predictions from these analyses were evaluated against data obtained from centrifuge model tests. The tests provided data over a wide range of strain levels, allowing predictions to be evaluated at both serviceability states and close to failure. This makes it possible to establish which features of the observed response of the wall/tunnel system can be reproduced by the each of the constitutive models over this wide range of strain levels, and how the behaviour predicted at small strain also influences the large strain response.

2. Centrifuge tests used as benchmark.

The benchmark for the numerical analyses is a series of centrifuge tests which were performed at City University London^{7, 8}. These tests were carried out on models reduced by a scale factor, N , equal to 160 and accelerated to 160g, following centrifuge scaling laws for length⁹. In the tests, a diaphragm wall was embedded into a model, constructed from Speswhite kaolin, close to a circular cavity of diameter, D , 50mm and cover to diameter ratio, C/D , equal to 1, as shown in Fig. 1. Image processing targets placed on the face of the model allowed tracking of the ground movements within the soil mass by the use of digital image analysis¹⁰. Pore pressures were also measured at discrete points in the model.

The diaphragm wall was modelled by means of an aluminium plate and the tunnel cavity was supported by a rubber bag inflated with compressed air. The inner air pressure was reduced during the test to simulate the tunnel excavation.

3. Numerical model.

The numerical analyses were conducted using CRISP¹¹, a finite element program in which both Modified Cam-clay and the 3-SKH model are implemented.

The shape and size of the mesh used in the numerical analyses represented a complete section through the physical model, being 550mm wide and 155mm high. The numerical analyses were conducted under plane strain conditions. The vertical boundaries were restrained horizontally to simulate the well greased boundaries of the centrifuge test and the base of the mesh is restrained both horizontally and vertically as

in the centrifuge model tests. The water table was fixed 2mm below ground level. A schematic drawing of the mesh is shown in Fig. 2.

The mesh consisted of 1329 nine-noded linear strain triangles including 3 nodes allowing pore pressure degrees of freedom. It represented the full cross section through the centrifuge model to account for the lack of symmetry caused by the presence of the wall on one side of the tunnel.

Extensive computational work was performed¹², which modelled the behaviour of several centrifuge models using both Modified Cam clay and the 3-SKH model. In order to compare the ability of the two constitutive models to predict the stress-strain behaviour of the overconsolidated clay for this boundary value problem, analyses of two representative centrifuge models have been selected and the results of these analyses will be discussed in this paper. One set simulated ground movements under greenfield conditions (without a diaphragm wall), the second set modelled the behaviour of the ground with a diaphragm wall embedded near the tunnel. The wall ($L = 70\text{mm}$, $t = 9.5\text{mm}$) was embedded at a horizontal distance of 50mm from the tunnel axis as shown in Fig. 1.

4. Material characterisation

The values for the parameters representing the soil properties that are used in the Modified Cam-clay and 3-SKH models have been taken from the literature and are given in Tables 1 and 2. These values resulted from a careful calibration of the two models during an extensive laboratory testing programme on Speswhite kaolin^{5, 13, 14, 15}.

The unit weight of the soil, γ , is 17.44 kN/m^3 .

The parameters λ^* and κ^* in Table 2 correspond, over an appropriate stress range, to the parameters λ and κ in Table 1 if the normal compression line and the unloading-reloading lines are defined in bi-logarithmic space¹⁶, $\ln(1+e) : \ln p'$.

The embedded aluminium wall has been modelled using six-noded linear strain triangles and an isotropic linear elastic material type, where Young's Modulus, E , is equal to 70 GPa, Poissons ratio is equal to 0.25 and the unit weight is 27 kN/m³.

5. Analysis Procedure

Table 3 describes how the loading history of the centrifuge model was reproduced in the numerical analyses, starting at the end of the initial consolidation stage under a press at $\sigma'_v = 350\text{kPa}$. For both models this is necessary to set up stresses around the tunnel cavity that are consistent with the inner support pressure and the appropriate g level; for the 3-SKH model this also ensures that an appropriate stress history has been generated. Consequently, the effective vertical stress at the start of the analyses was 350 kPa and constant with depth. The initial horizontal effective stress was calculated by using a constant value of $K_o = 1 - \sin\phi'$, where ϕ' is calculated from M assuming conditions of triaxial compression.

The analysis was carried out under drainage conditions simulated using coupled consolidation, with drainage to the base only. In the first three stages of the analysis (Phases 1 – 3 in Table 3) the following steps were undertaken; the surcharge on the surface of the mesh was reduced by 200kPa to simulate swelling in the press, the gravitational field was increased to the correct level and the surcharge at ground surface was reduced to zero to simulate conditions on the centrifuge swing at 160g, the tunnel

elements were removed and a supporting pressure applied to simulate the state of the tunnel prior to the reduction of tunnel pressure. At this stage, the computed variation in the equilibrium vertical effective stress and pore pressure, at the centre of the mesh, were as shown in Fig. 3. These stresses should be consistent with the state of the model soil when pore pressure equilibrium is reached on the centrifuge under 160g. For the model with a diaphragm wall, aluminium elements were substituted for the soil elements corresponding to the position of the wall (Phase 4 in Table 3).

In Fig. 4a the profile of p'_c with depth is shown for both models; this is the mean effective stress at the intersection between the state boundary surface and the normal compression line and represents the size of the projection of the state boundary surface along an elastic wall. As Modified Cam clay does not allow yielding during unloading, the value of p'_c is constant with depth and equal to the initial value, which defines the elastic wall passing through the point on the K_0 -compression line defined by the maximum vertical stress of 350kN/m^2 . On the contrary, p'_c varies with depth in the 3-SKH analysis, reducing near the ground surface. This is because the model allows negative plastic volumetric strain inside the state boundary surface during swelling moving the state of the soil to elastic walls defined by lower values of p'_c and corresponding to higher values voids ratio, Fig 4b. The greatest differences between the profiles of earth pressure coefficient K_0 predicted by the two models (Fig 4c) occurs above the tunnel. For the first 15 mm (2.4 m at prototype scale) below the surface both models predict values of K_0 which are significantly higher than would occur in practice. The undrained resistance s_u , which is a common input parameter in finite element analyses performed using total stresses and undrained conditions, has been calculated from the void ratio e and critical state parameters, using equation (1):

$$s_u = \frac{1}{2} M \exp \left[\frac{\Gamma - e - 1}{\lambda} \right] \quad (1)$$

The undrained shear strength profile can also be assessed by means of the expression proposed by Ladd & Edgers¹⁷ and modified according to Mesri¹⁸:

$$s_u = 0.22 \sigma'_v OCR^{0.8} \quad (2)$$

As can be observed in Fig. 4d, the undrained shear strength calculated from the voids ratios predicted by the 3-SKH model is closer to the empirical prediction (2) than that computed by the Modified Cam clay model. The latter significantly underestimates the void ratio e and therefore over predicts the undrained shear strength of the soil above the tunnel.

In the last stage of the analysis, the pressure inside the cavity was reduced to zero. The time period used in the consolidation analysis for this stage was 120 seconds, which is approximately the duration of this process in the centrifuge tests. The numerical analyses use model dimensions so these time periods should be the same to simulate the consolidation process correctly. Because of this relatively short time period, even though the analysis allowed the soil to consolidate, the computed response was essentially undrained.

6. Comparison between numerical and experimental results

In the following, the results of the numerical analyses will be compared to the test results in terms of soil displacements near ground surface, wall displacements and stresses around the tunnel.

6.1 Settlements induced at the ground surface during reduction of tunnel support pressure

In Fig. 5 the maximum settlements, $S_{v,max}$, observed at a depth $z = -5$ mm are plotted against percentage reduction in tunnel support pressure, $-\Delta\sigma_T/p_o$, where p_o is 190kPa, the initial support pressure in the tunnel. The computed movements are compared to the experimental observations for the model tunnel without a diaphragm wall.

The Modified Cam clay model predicts a quasi-linear variation of settlement with decreasing pressure until about $-\Delta\sigma_T/p_o = 50\%$, unlike the curve predicted by the 3-SKH model which appears clearly non-linear from the beginning. The percentage reduction in pressure at which deformation appears to increase significantly, denoting collapse, is also different: in the analysis performed using the 3-SKH model this occurs at around $-\Delta\sigma_T/p_o = 80\%$, whereas the settlement calculated at the same pressure in the analysis with Modified Cam clay is still low and large deformations only occur at a pressure reduction of about 95%. This behaviour is consistent with the computed stress-paths in the area around the tunnel. As will be shown later, the stress paths around the tunnel evolve inside the state boundary surface and consequently whilst Modified Cam clay only computes elastic strains with a constant stiffness, the 3-SKH model allows plastic strains to develop and stiffness to decrease. Looking at the settlements measured during the test, it is evident that the deformations predicted using the 3-SKH model are closer

to the physical results than those predicted using Modified Cam clay: the curve predicted by the 3-SKH model is very similar to the experimental curve until about $-\Delta\sigma_T/p_o = 60\%$. After this point, the cavity approaches collapse in the test while the numerical model is still showing hardening. It should also be noted that the larger reduction of support pressure allowed by Modified Cam clay is consistent with the higher available undrained strength predicted by this model before the ‘excavation’ stage (Fig. 4d).

Also for the model without a diaphragm wall, Fig. 6 shows percentage reduction in tunnel support pressure $-\Delta\sigma_T/p_o$ plotted against volume loss V' . The figure clearly shows that again the response predicted initially by Modified Cam clay is almost linear while the 3-SKH model prediction is closer to the non-linear behaviour observed in the test. Initially, $-\Delta\sigma_T/p_o$ from 0 to 20%, the relationship between V' and reduction in tunnel support pressure predicted by the 3-SKH model is fairly similar to that observed. However, for $-\Delta\sigma_T/p_o$ from 20% to 60%, the effect of predicting a wider surface settlement profile than that observed in the tests, see later, means that the 3-SKH model predicts a much greater volume loss at an equivalent tunnel support pressure, than was measured in the tests. At changes in support pressure greater than 60%, the tunnel is nearing failure and the development of this failure is not well reproduced by the small strain finite element formulation, such that volume loss will be under predicted. In the range of V' between 10% and 30%, the average value of support pressure σ_T is about 65 kPa in the test, 75 kPa according to the 3-SKH model and 35 kPa according to the Modified Cam clay model.

The difference in support pressure σ_T in the range of $V' = 10\%$ to 30% is related to the different values of s_u . In fact at a given volume loss the stability ratio, N , which is

defined as $(p_o - \sigma_T)/s_u$ should assume similar values both in the test and in the two numerical models, as shown in Table 4. Average values of s_u for the soil in the tunnel cover have been calculated from the data shown in Fig.4 and used together with the aforementioned values of σ_T to calculate these stability ratios.

In Figs. 7 and 8 the settlement of the wall $S_{v,wall}$ and the volume loss V' for the model with a diaphragm wall are plotted against percentage change in tunnel support pressure. Over the % change in support pressure for which data for the 3-SKH model analyses are available, the values predicted by this model appear closer to the experimental measurements than those predicted using Modified Cam clay. However both models significantly underpredict wall movements at values of $-\Delta\sigma_T/p_o$ corresponding to failure in the centrifuge test. At failure, the analysis using 3-SKH model was stopped as computational errors started to increase, making results from the later time increments unreliable; however, the trend of the curve indicates that this model under predicted the value of the experimental tunnel support pressure at collapse, by much less than the Modified Cam clay model. The latter predicts that the unsupported cavity will not collapse, which is completely different from the behaviour observed in the test, where the model tunnel with a wall collapsed before the model tunnel without wall (i.e. at a lower pressure change). Computed curves of volume loss against change in tunnel support pressure presented in Fig. 8 are very similar to those in Fig. 6, indicating that the overall response of the system to the tunnel excavation computed by both the 3-SKH model and Modified Cam clay is not significantly affected by the presence of the wall until the tunnel is near to failure, where computational difficulties dominate.

6.2 Profiles of near surface displacements

The settlements and the horizontal displacements measured and computed at a depth $z = -5\text{mm}$ and at $\Delta\sigma_T/p_o \cong -40\%$ for the model with a wall are compared with the experimental measurements in Fig. 9.

Both analyses over predict the far field settlements and the analysis using the 3-SKH model also predicts greater maximum settlements than those observed in the test.

The distribution of the surface settlements predicted by the latter is much closer to that observed than the predictions using the Modified Cam clay model. In particular, the 3-SKH model is able to reproduce the large vertical movement of the wall observed in the test. This seems to be largely dependent on the stress state predicted in the area between the wall and the cavity. However, the settlement trough predicted by the 3-SKH model is wider than that measured and predicted by Modified Cam clay. The width of the settlement trough above a tunnel predicted by the 3-SKH model is known to depend on the recent stress history applied to the soil. Wider settlement troughs result when the most recent stress history is volumetric swelling, a phenomenon first described by (Find paper). This is the stress history of the overconsolidated soil in the centrifuge test being analysed. More accurate predictions might well be obtained by optimising model material parameters, but for consistency this was not undertaken here. The 3-SKH model is also less successful in predicting the pattern and magnitude of the horizontal movements. This is caused by the detail of the interface between the wall and the soil. In the analyses, because this is perfectly rough and there is insufficient shear deformation at the interface, horizontal displacements result from continuum soil elements being dragged down with the wall. In the model test there is obviously a more discontinuous shear zone at this interface, which results in less horizontal displacement.

6.3 Stress paths around the tunnel and between the tunnel and the diaphragm wall tip

An important measure of the success of a constitutive model is whether it is able to reproduce different stress-strain paths from those which have been used to calibrate its mechanical parameters.

The stress change during the undrained ‘excavation’ path in the centrifuge tests has been monitored using a pair of pore pressure transducers: one located close to the tunnel cavity (PPT1), the second (PPT2) far away from it.

In Fig. 10 the pore pressures measured at the two locations (PPT1 and PPT2) in each test have been plotted together with the numerical predictions. The clear jumps in the experimental curves for PPT1 correspond to the tunnel collapse.

It can be observed that the 3-SKH model predictions reproduce the characteristics of the observed response more closely than the Modified Cam clay model. In fact, the latter does not predict significant pore pressure change until yielding occurs, as the response is elastic until a clear kink in the curve, denoting the yield point. After that, the pore pressure quickly decreases due to plastic dilatant behaviour. Conversely, as noted earlier, yielding is predicted at low changes in support pressure by the 3-SKH model, even for an unloading path, due to its kinematic hardening formulation, resulting in predictions which are, at least initially, closer to those measured.

The computed stress-paths for some integration points around the tunnel are shown in Fig. 11 in a normalised q - p' plane. The variables p' and q are defined in the general stress state as $p' = I_1/3$ and $q = \sqrt{3J_2}$, where I_1 is the first stress tensor invariant and J_2 is the second stress deviator tensor invariant. The variable p'_0 defines the size of the yield surface in Modified Cam clay and of the bounding surface in the 3-SKH model.

The Modified Cam clay model predicts constant p' stress-paths around the tunnel consistent with an elastic soil as the initial stress state lies well inside the yield surface. On the other hand, the 3-SKH model predicts an increase in p' , caused by negative excess pore pressures arising because the model would like to dilate.

At all the points which have been monitored around the cavity, apart from point B which is discussed later, the Modified Cam clay model predicts a very slight increase in the total mean stress, p , in the early stages of the excavation, with an elastic increase of pore pressure u at a constant mean effective stress p' , until the yield surface is reached. On the contrary, the 3-SKH model always predicts a decrease in the total mean stress p and an increase in the effective mean stress p' together with a decrease in pore pressure u . The deviator stress q sometimes decreases towards the critical state after reaching a peak value for predictions using Modified Cam clay while it always increases for predictions using the 3-SKH model.

It seems that the behaviour of corresponding integration points in symmetrical positions around the tunnel is very similar, except for points A and B: point B belongs to a triangular element beneath the diaphragm wall tip, point A is the corresponding point on the other side of the tunnel.

The stress-strain behaviour of these two integration points is described in Fig. 12. The variable ε_s in this figure is the deviator strain and it is computed as $\varepsilon_s = \left(2/\sqrt{3}\right)\sqrt{E_2}$, where E_2 is the second strain deviator tensor invariant.

The computed values of p' at point B increase in the analyses using the Modified Cam clay model, unlike those at point A: this demonstrates the influence of the self weight of the diaphragm wall on the evolution of the stress in the area between the wall tip and the

tunnel, while the tunnel support pressure is decreasing. This effect is also computed by the analyses using the 3-SKH model. Nevertheless, according to the Modified Cam clay model positive excess pore pressures are predicted in the first stages of excavation, as a consequence of the increase in p in elastic soil, whereas negative excess pore pressures are predicted as soon as the excavation starts, when the 3-SKH model is used.

It is clear from Fig. 12 that the main differences in the predicted behaviour of the soil between the tunnel and the wall tip arise in the early stages of the excavation. This explains why, as shown in Fig. 9, the settlement trough at $\Delta\sigma_T/p_o \cong -40\%$ is not well predicted by the Modified Cam clay model.

7. Discussion

The problem analysed highlights the inability of the Modified Cam clay model to predict realistic patterns of movements in overconsolidated soils, in this case this is a particular issue in the vicinity of the wall.

The use of critical state models requires the definition of soil parameters under drained conditions. Careful consideration is needed to ensure that these will be appropriate when analysing the short term behaviour of the soil. A key issue is modelling in an appropriate way the initial undrained strength profile, as this is related to the stress level at which yielding occurs. This is critical when assessing the stability of soil structures, but it can also be very influential on the pre-failure behaviour of the soil, depending on the formulation of the constitutive model.

The investigation into the stress-strain behaviour of the integration points beneath the diaphragm wall tip (*cf.* Fig. 12) has shown that according to the Modified Cam clay model the soil is largely in an elastic state, as the stress moves inside the yield surface,

developing small positive excess pore pressures until the deviator stress change exceeds about 100 kPa. The previous stress history generated a larger yield surface than in the 3-SKH model analyses and yield only occurs in the Modified Cam clay model at the boundary surface, defining a relatively high value for the undrained shear strength. The 3-SKH model, on the contrary, allows for shrinkage of the elastic region, due to its nested yield surfaces inside the state boundary surface. This permits a more accurate prediction of the available shear strength in the short term for overconsolidated clay, as shown in Fig. 4.

Moreover, it also allows the simulation of the non-linear stiffness of the soil during the early stages of the undrained stress release around the tunnel cavity, as shown in Fig. 6. Although the 3-SKH model is able to reproduce the non-linear response of the soil, the maximum surface settlement is higher than that measured in the test at the same support pressure, as also observed by other Authors modelling the small strain stiffness of soil for comparable stress-paths¹⁹. Moreover, the calculated settlement troughs are wider, resulting in larger values of V' than observed.

In general, good predictions of the response of the tunnel wall system during the early stages of excavation are very important, as strain levels around real tunnels are very low due to the sophisticated techniques now commonly used to excavate and support tunnels in soft ground. However, these analyses also show that it not sufficient just to reproduce the small strain non-linearity of deformations. The settlement profiles (*cf.* Fig. 9) are also significantly affected by overestimation of the undrained shear strength by the Modified Cam clay model, which reduces the degree of shear mobilisation around the diaphragm wall, allowing better support than was observed during the test.

8. Conclusions

The paper compares the performance of the Modified Cam clay model and the Three-Surface Kinematic Hardening model when used to solve the boundary value problem of a diaphragm wall interacting with a tunnel excavation. Experimental results from centrifuge tests are used as a benchmark to evaluate the finite element analyses.

The numerical computations have been reviewed and compared in terms of ground and wall movements at or near surface and stress-strain behaviour around the tunnel and at the base of the wall.

Simpson *et al.*²⁰ demonstrated the importance of modelling the non-linearity of soil stiffness at small strains to analyse serviceability limit states of soil-structure interaction problems. Therefore the improved prediction obtained using the 3-SKH model compared to the Modified Cam clay model is perhaps not surprising and at small strains patterns of deformation are still more widespread than observed in the centrifuge tests. Recent efforts to improve the small-strain stiffness formulation of the 3-SKH model by Grammatikopoulou *et al.*²¹ have ensured a smooth transition from elastic to elastoplastic behaviour, which might help to improve the predictions of the 3-SKH model at very low strain, where it over predicts the ground displacements due to the abrupt drop of stiffness which occurs as soon as yielding starts. Nevertheless, this improvement in the prediction of the shear modulus decay is in a range of deformation which is more typical of the serviceability state of a retaining structure (0.01% to 0.1%) rather than a tunnel (0.1% to 1%)²².

However, it is the different behaviour of the two constitutive models near failure which is most significant, the analyses demonstrating that the large strain response is highly dependent on the small strain formulation. In particular, at large strains, predictions

obtained using the 3-SKH model are in many cases very close to the observed behaviour, and always much closer than the Modified Cam clay results. The stress paths computed at several integration points around the tunnel and at the wall tip provided evidence that the kinematic formulation of the 3-SKH model allows the size of the boundary surface, which regulates large strain plastic deformations, to be set up correctly. Such an issue is important as it avoids the overestimation of undrained shear strength dry of critical state and improves predictions near failure.

List of symbols

A, m, n , parameters defining the elastic shear modulus in the 3-SKH model;
 C , soil cover above the tunnel;
 D , tunnel diameter;
 E_2 , second strain deviator tensor invariant;
 $e, ,$ void ratio
 e_{cs} , reference void ratio on critical state line when $p'=1$ kPa;
 I_1 , first stress tensor invariant;
 J_2 , second stress deviator tensor invariant;
 k_v, k_h , permeability of soil in vertical and horizontal direction;
 L , length of the diaphragm wall;
 N , stability ratio;
 p, p' , total and effective mean stress;
 p_o , overburden pressure around cavity;
 p'_c , mean effective pressure at the intersection of the current swelling line with the normal compression line;
 q , deviator stress
 S , ratio of the size of the yield surface to the size of the history surface in the 3-SKH model;
 S_v , settlement induced by tunnel excavation;
 T , ratio of the size of the history surface to the size of the bounding surface in the 3-SKH model;
 t , thickness of the diaphragm wall;
 u , pore pressure;
 V' , percentage volume of the settlement trough, in undrained conditions it coincides with the 'volume loss';
 $-\Delta\sigma_T/p_o$, relative change in support pressure during the simulated tunnel excavation;
 ε_s , deviator strain
 κ^* , slope of unload-reload lines in $\ln v: \ln p'$ plane;
 λ^* , slope of isotropic compression line in $\ln v: \ln p'$ plane;
 ψ , exponent in the hardening function of 3-SHK model;
 σ_T , cavity support pressure;
 M , slope of critical state line in $q: p'$ plane.

References

1. Zdravkovic L. and Carter J. Contribution to Géotechnique 1948-2008: Constitutive and numerical modelling. *Géotechnique*, 2008; 58(5): 405-412.
2. Mroz Z., Norris V.A. and Zienkiewicz O.C. An anisotropic hardening model for soils and its application to cyclic loading. *Int. J. Numer. Analyt. Meth. Geomech.* 1978; 2(3): 203-221.
3. Mroz Z., Norris V.A. and Zienkiewicz O.C. Application of an anisotropic hardening model in the analysis of elasto-plastic deformation of soils. *Géotechnique* 1979; 29(1):1-34.
4. Roscoe K.H. and Burland J.B. On the generalised stress-strain behaviour of a 'wet' clay, in *Engineering plasticity*, Heyman & Leckie (eds.) 1968. p. 535-609.
5. Stallebrass S.E. Modelling the effect of recent stress history on the deformation of overconsolidated soils. PhD Thesis. City University, London, 1990.
6. Stallebrass S.E. and Taylor R.N. The development and evaluation of a constitutive model for the prediction of ground movements in overconsolidated clay. *Géotechnique*, 1997; 47(2): 235-253.
7. Bilotta E. and Taylor R.N. Centrifuge modelling of tunnelling close to a diaphragm wall. *Int. J. of Physical Modelling in Geotechnics* 2005; 5(1): 27-41.
8. Bilotta E. Use of diaphragm walls to mitigate ground movements induced by tunnelling. *Géotechnique* 2008; 58(2): 143-155.
9. Schofield A.N. Cambridge geotechnical centrifuge operations, *Géotechnique* 1980; 30(3): 227-268.
10. Taylor R.N., Grant R.J., Robson S. & Kuwano J. An image analysis system for determining plane and 3-D displacements in soil models, *Centrifuge '98* (Kimura, Kusakabe & Takemura eds). Rotterdam: Balkema., 1998. p. 73-78
11. Britto A.M. and Gunn M.J. *Critical State Soil Mechanics via Finite Elements*, Ellis Horwood, Chichester, 1987.
12. Bilotta E. Diaphragm walls to mitigate ground movements induced by tunnelling. Experimental and numerical analysis. PhD Thesis. Universities of Roma La Sapienza and Napoli Federico II, 2004.
13. Al-Tabbaa A. Permeability and stress-strain response of Speswhite kaolin, PhD Thesis, University of Cambridge, 1987.
14. Morrison P.R.J. Performance of foundations in a rising groundwater environment, PhD Thesis, City University, London, 1994.
15. Viggiani G.M.B. Small strain stiffness of fine grained soils. PhD Thesis. City University, London, 1992.
16. Butterfield R. A natural compression law for soils, *Géotechnique*, 1979; 29 (4): 469-480.
17. Ladd C.C. and Edgers L. Consolidated-undrained direct-simple shear tests on saturated clays, MIT, Dept. of Civil Eng. Research report, R72-82, 1972.
18. Mesri G. Discussion: New design procedure for stability of soft clays, *Proc. ASCE, Journal of the Geotechnical Engineering Division* 1975; 101(GT4): 409-412.
19. Gunn M.J. The prediction of surface settlement profile due to tunnelling. In: *Predictive soil mechanics*, London: Thomas Telford, 1993. p. 304-316.

20. Simpson B., O'Riordan N.J. and Croft D.D. A computer model for the analysis of ground movements in London Clay. *Géotechnique* 1979; 29(2). 149-175.
21. Grammatikopoulou A., Zdravkovic L. and Potts D. General formulation of two kinematic hardening constitutive models with a smooth elastoplastic transition. *Int. J. of Geomechanics (ASCE)* 2006; 6(5): 291-302.
22. Mair R.J. Unwin Memorial Lecture 1992. Developments in geotechnical engineering research: application to tunnels and deep excavations. *Proc. ICE, Civ. Engng* 1993; 93(Feb): 27-41.

List of captions

Figures

Figure 1 – Front picture, elevation (a) and plan (b) of the model.

Figure 2 - Sketch of the mesh.

Figure 3 – Vertical effective stresses and pore pressure after removing the tunnel soil elements and applying the support pressure.

Figure 4 – Comparison between 3-SKH model and Modified Cam clay model when there is no wall, before decreasing support pressure.

Figure 5 - Maximum settlement at depth –5mm vs percentage change in tunnel support pressure in both numerical and physical models without wall.

Figure 6 - Percentage change in tunnel support pressure vs volume loss in both numerical and physical models without wall.

Figure 7 - Wall settlement vs percentage change in support pressure in both numerical and physical models with wall.

Figure 8 - Percentage change in tunnel support pressure vs volume loss in both numerical and physical models with wall.

Figure 9- Comparison between computed and measured displacements at surface.

Figure 10 - Measured and predicted pore pressures at the locations of PPT1 and PPT2.

Figure 11 - Stress paths at selected integration points around the tunnel (Modified Cam clay vs 3-SKH.)

Figure 12 - Stress-strain behaviour in the point B under the wall and in the symmetrical point A.

Tables

Table 1 - Soil parameters for the Modified Cam clay model (Morrison, 1994).

Table 2 - Soil parameters for the 3-SKH model (Stallebrass, 1990; Viggiani, 1992.)

Table 3 – Phases of analysis and corresponding experimental steps

Table 4 – Stability ratios for $V'=10\%$ to 30% .

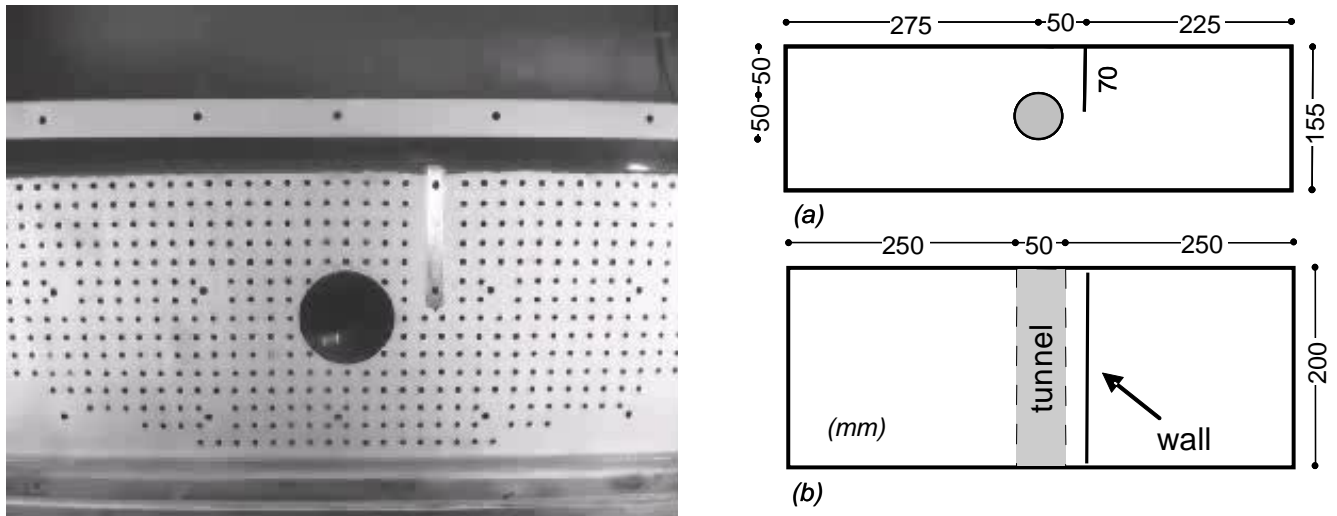


Figure 1 – Front picture, elevation (a) and plan (b) of the model

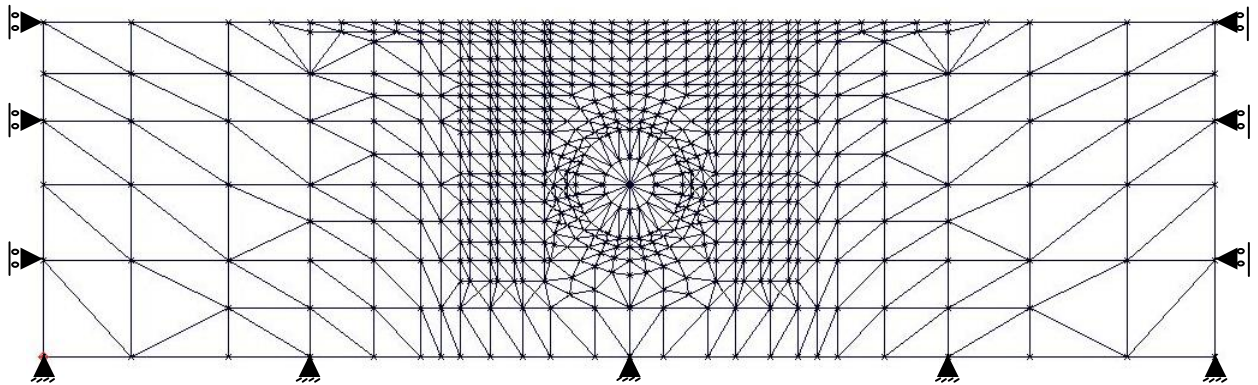


Figure 2 - Sketch of the mesh.

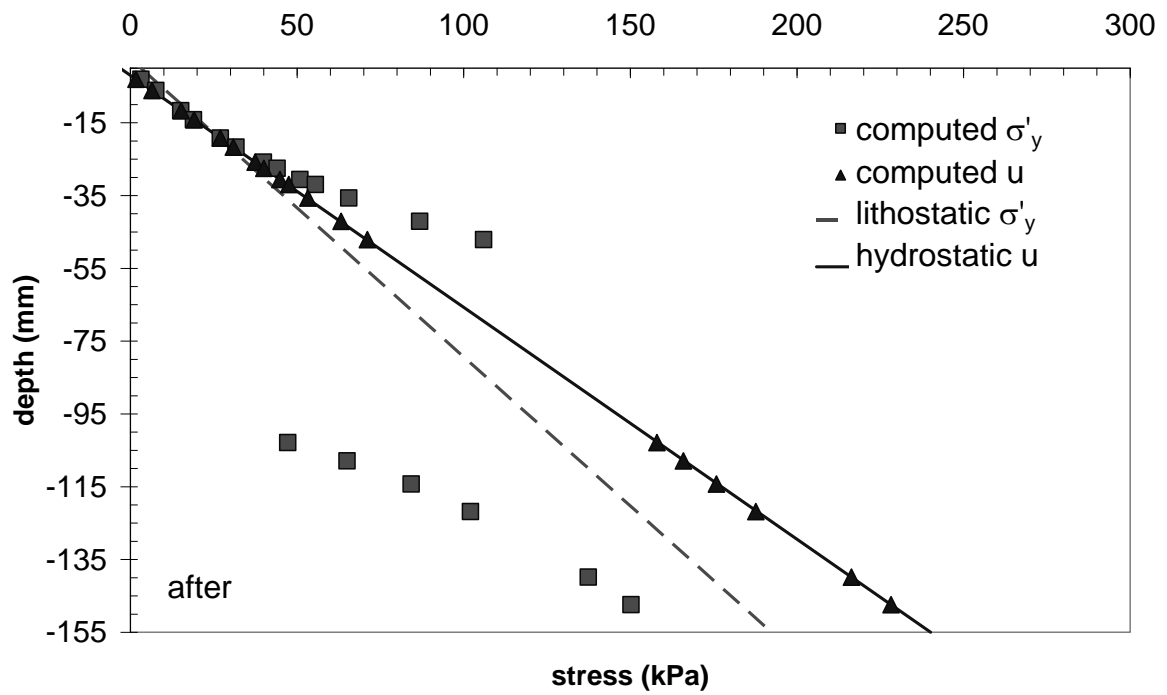


Figure 3 – Vertical effective stresses and pore pressure after removing the tunnel soil elements and applying the support pressure

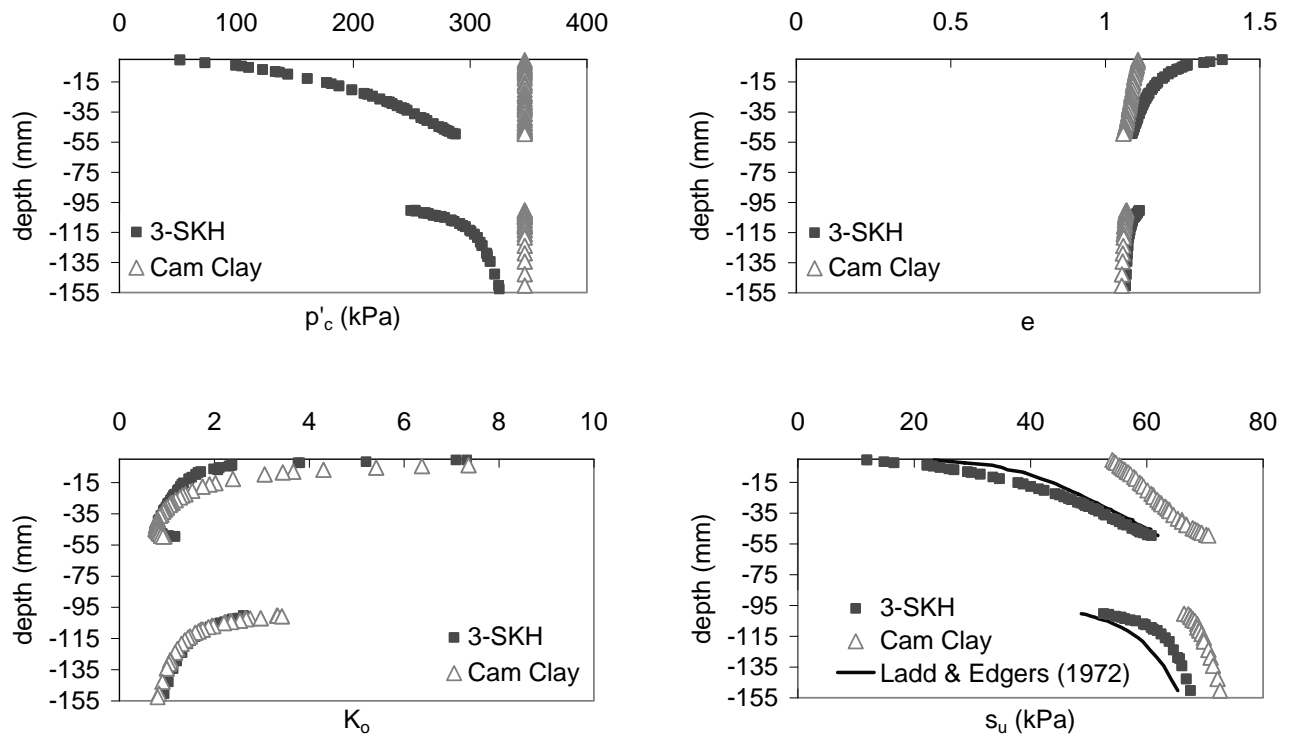


Figure 4 – Comparison between 3-SKH model and Modified Cam clay model when there is no wall, before decreasing support pressure

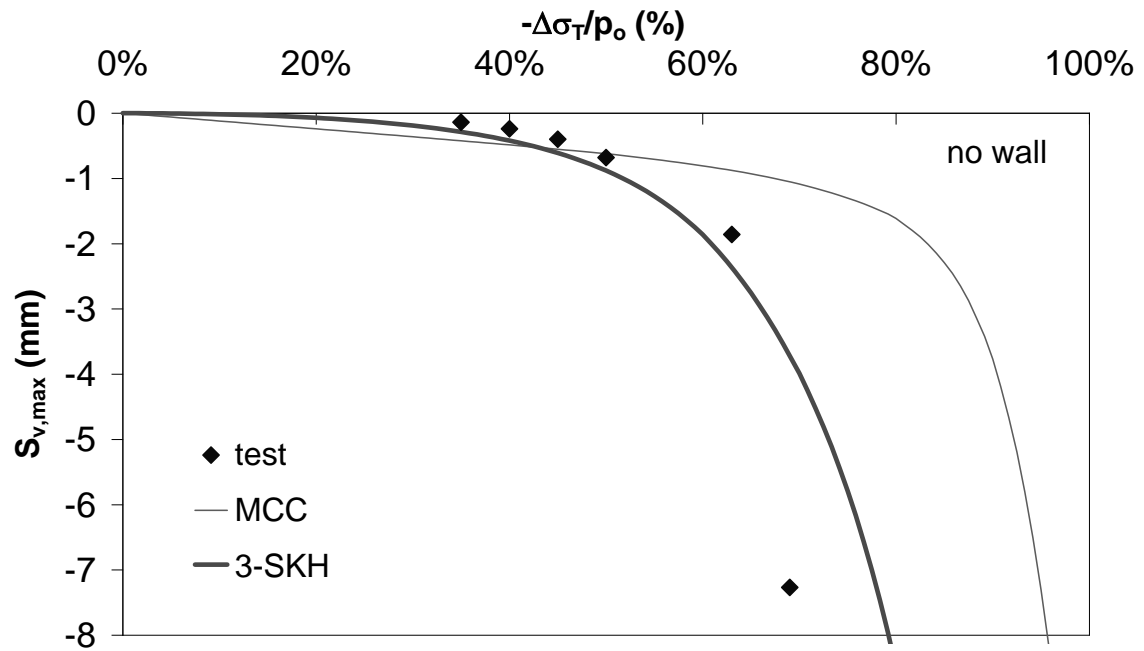


Figure 5 - Maximum settlement at depth -5mm vs percentage change in support pressure in both numerical and physical models without wall.

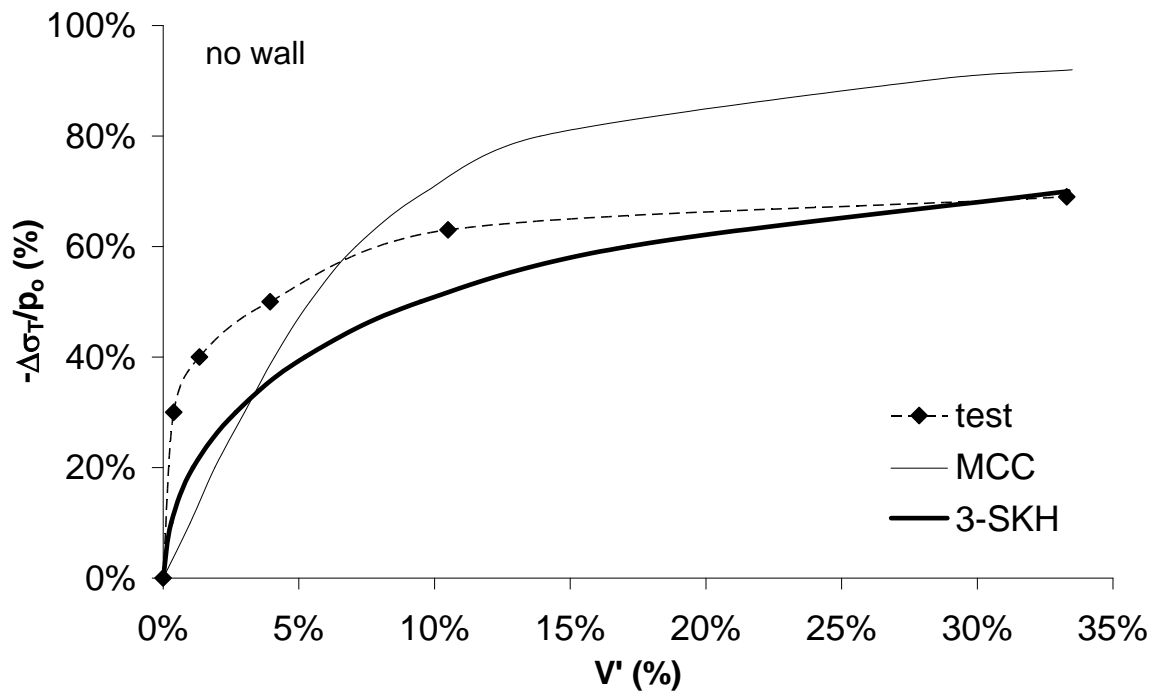


Figure 6 - Percentage change in tunnel support pressure vs volume loss in both numerical and physical models without wall.

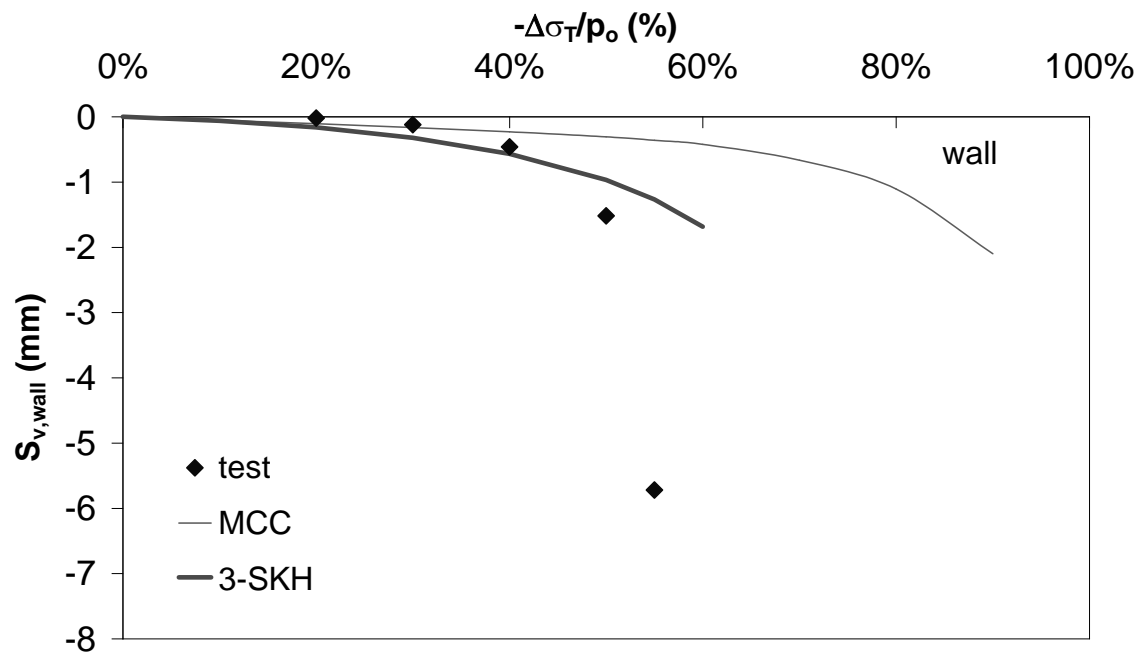


Figure 7 - Wall settlement vs percentage change in support pressure in both numerical and physical models with wall.

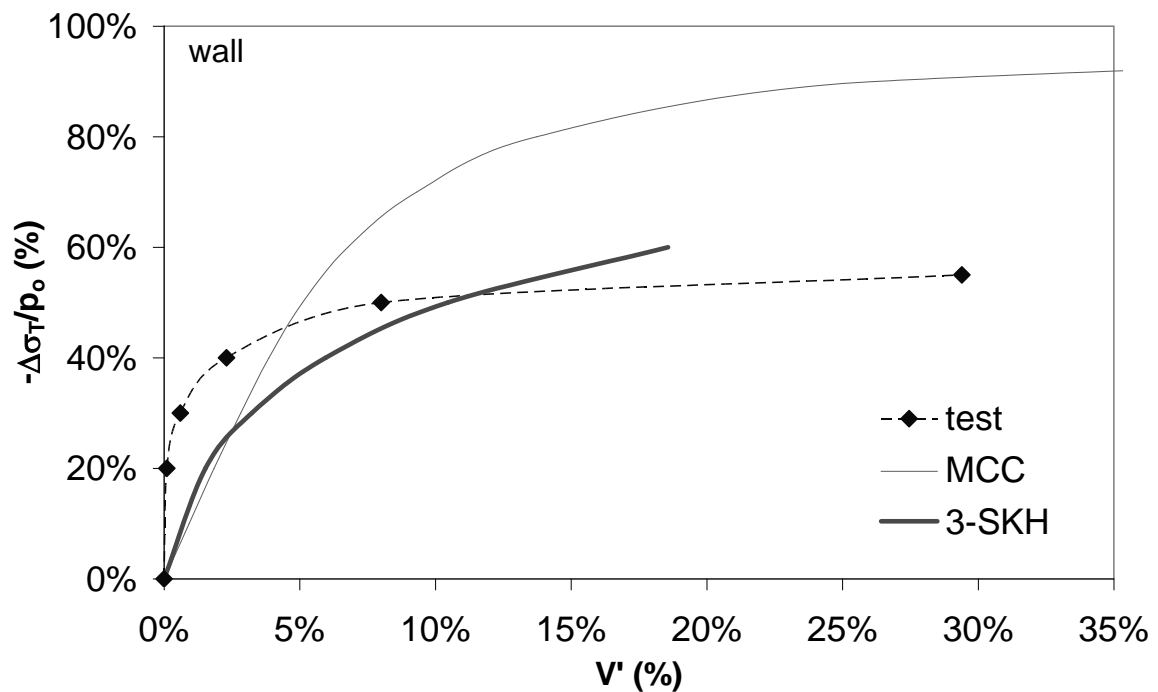


Figure 8 - Percentage change in tunnel support pressure vs volume loss in both numerical and physical models with wall.

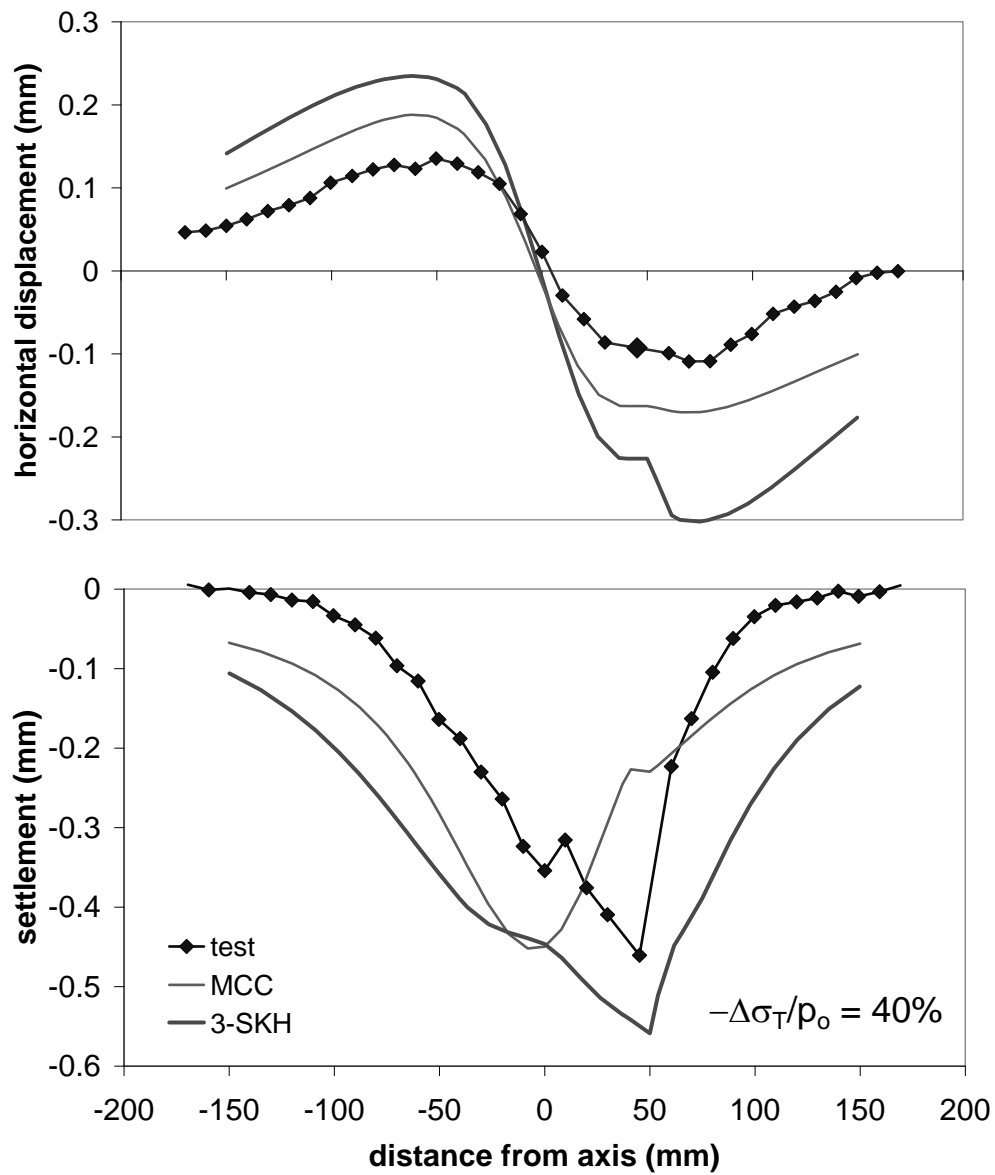


Figure 9- Comparison between computed and measured displacements at surface

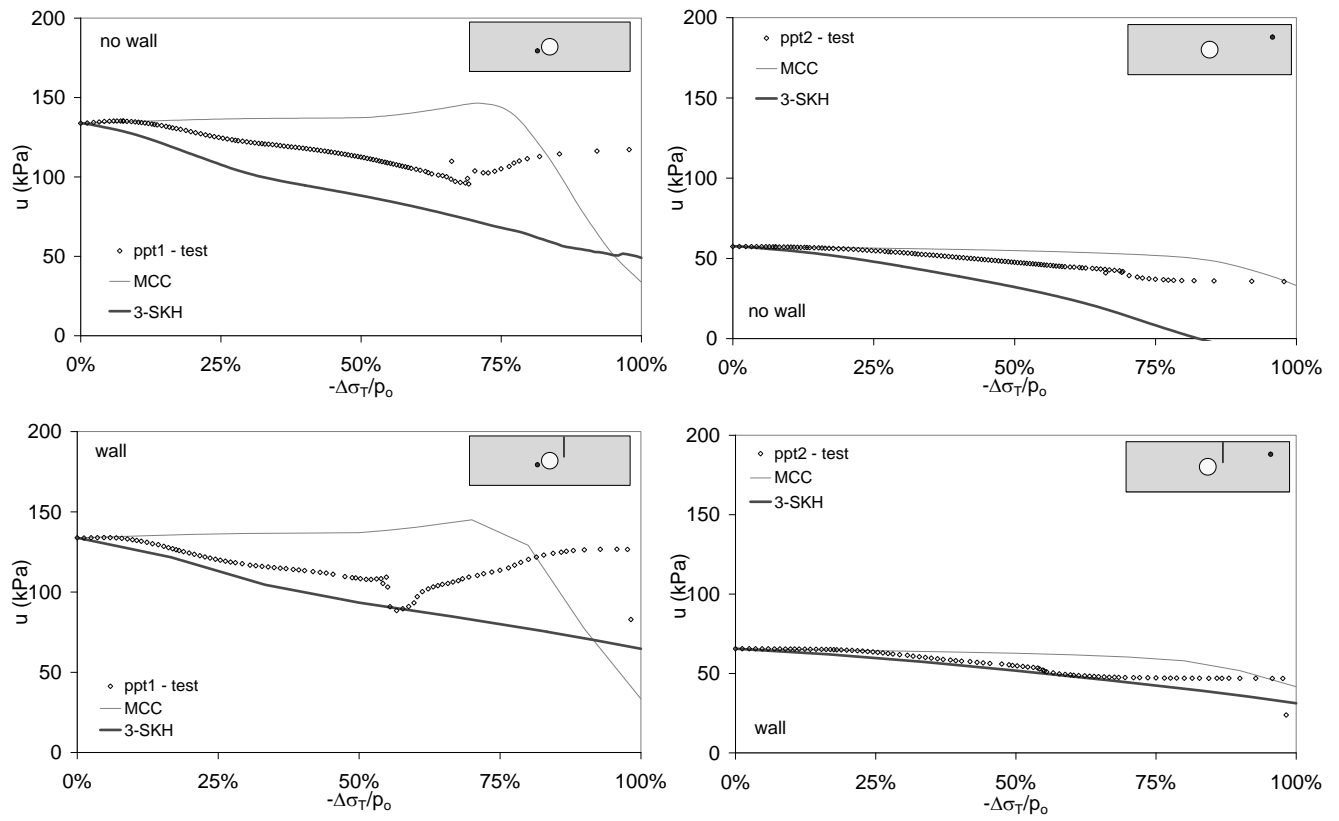


Figure 10 - Measured and predicted pore pressures at the locations of PPT1 and PPT2.

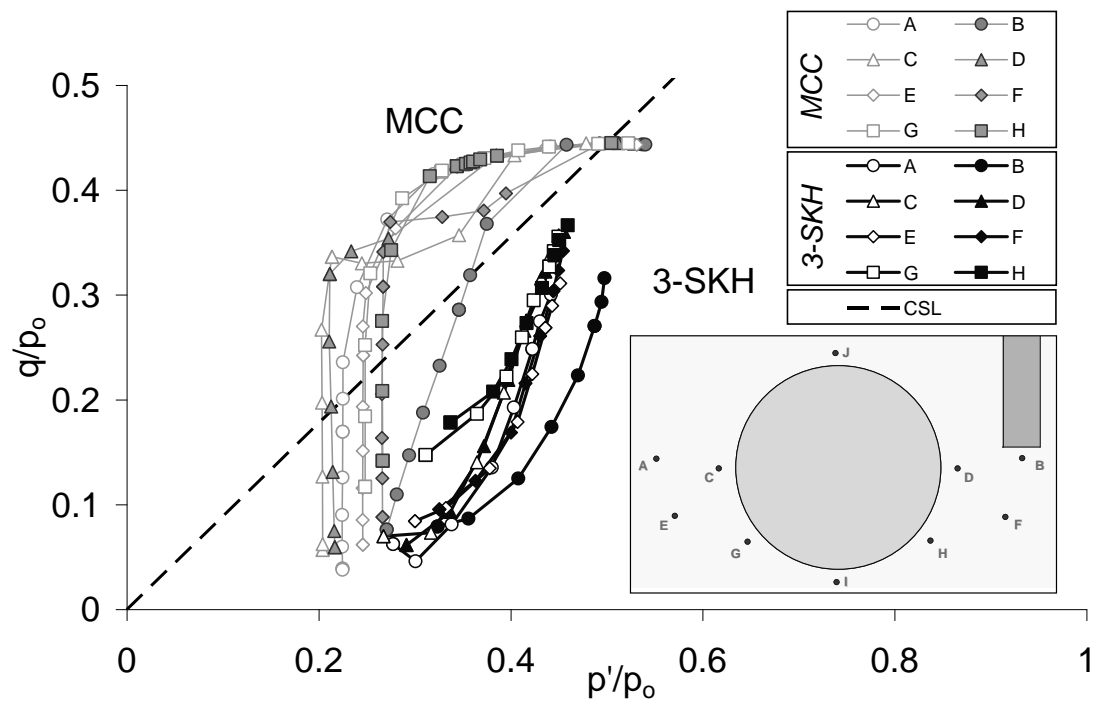


Figure 11 - Stress paths at selected integration points around the tunnel (Modified Cam clay vs 3-SKH)

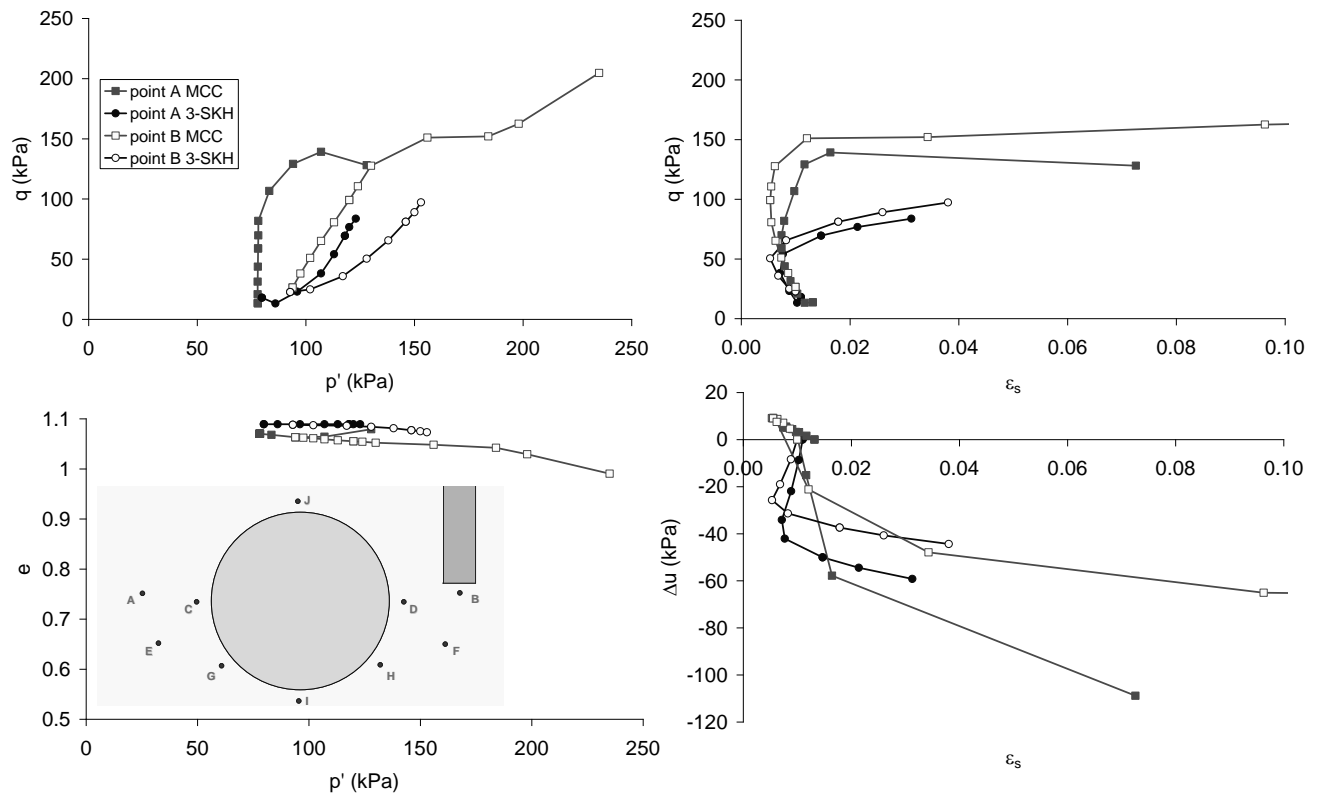


Figure 12 - Stress-strain behaviour in the point B under the wall and in the symmetrical point A

Table 1 - Soil parameters for the Modified Cam clay model ([13], [14])

M	λ	e_{cs}	κ	ν	k_v (mm/s)	k_h (mm/s)
0.89	0.18	1.97	0.035	0.3	0.58E-6	1.58E-6

Table 2 - Soil parameters for the 3-SKH model ([5], [13], [15])

M	λ^*	e_{cs}	κ^*	T	S	ψ	A (kPa)	m	n	k_v (mm/s)	k_h (mm/s)
0.89	0.073	1.994	0.005	0.25	0.08	2.5	1964	0.65	0.2	0.58E-6	1.58E-6

Table 3 – Phases of analysis and corresponding experimental steps

	Numerical modelling	Experimental activity
<i>Initial state</i>	Initial effective vertical equal to 350 kPa and constant with depth; $K_o = 1 - \sin \phi'$ Stresses in equilibrium with applied surcharge of 350kPa.	Soil sample under consolidometer at 350 kPa (full consolidated).
<i>Phase 1</i>	Surcharge of 200 kPa removed from the mesh surface (consolidation, very high time interval).	Soil sample unloaded in the consolidometer at 150 kPa (full consolidated);
<i>Phase 2</i>	Gravity multiplier increased to 160, remainder of surcharge removed (consolidation, very high time interval)	Extraction of the strong box from the consolidometer and model making (nearly undrained)
<i>Phase 3</i>	Elements of soil in the cavity removed and pressure of 190 kPa applied at the cavity boundary.	Model accelerated up to 160 g and air pressure in the tunnel increased to 190 kPa at the same time (full consolidation in flight).
<i>Phase 4</i>	Wall elements activation (in the model with wall)	
<i>Phase 6</i>	Pressure inside the cavity reduced to zero (consolidation, same time period as in test).	Pressure inside the cavity reduced to zero (nearly undrained).

Table 4 – Stability ratios for $V'=10\%$ to 30%

	<i>TEST (Eq. 2)</i>	<i>Modified Cam clay</i>	<i>3-SKH</i>
<i>average s_u (kPa)</i>	48	64	43
<i>N</i>	2.6	2.4	2.7